The effects of primordial non-Gaussianity on the cosmological reionization

D. Crociani,[1,2]⋆ L. Moscardini,[1,2]⋆ M. Viel[3,4]⋆ and S. Matarrese[5,6]⋆

[1]*Dipartimento di Astronomia, Università di Bologna, via Ranzani 1, I-40127 Bologna, Italy*
[2]*INFN/National Institute for Nuclear Physics, Sezione di Bologna, viale Berti Pichat 6/2, I-40127 Bologna, Italy*
[3]*INAF – Osservatorio Astronomico di Trieste, Via G.B. Tiepolo 11, I-34131 Trieste, Italy*
[4]*INFN/National Institute for Nuclear Physics, Sezione di Trieste, Via Valerio 2, I-34127 Trieste, Italy*
[5]*Dipartimento di Fisica, Università di Padova, Via Marzolo 8, I-35131 Padova, Italy*
[6]*INFN/National Institute for Nuclear Physics, Sezione di Padova, Via Marzolo 8, I-35131 Padova, Italy*

ABSTRACT

We investigate the effects of non-Gaussianity in the primordial density field on the reionization history. We rely on a semi-analytic method to describe the processes acting on the intergalactic medium (IGM), relating the distribution of the ionizing sources to that of dark matter haloes. Extending previous work in the literature, we consider models in which the primordial non-Gaussianity is measured by the dimensionless non-linearity parameter f_{NL}, using the constraints recently obtained from cosmic microwave background data. We predict the ionized fraction and the optical depth at different cosmological epochs assuming two different kinds of non-Gaussianity characterized by a scale-independent and a scale-dependent f_{NL} and comparing the results to those for the standard Gaussian scenario. We find that a positive f_{NL} enhances the formation of high-mass haloes at early epochs when reionization begins, and, as a consequence, the IGM ionized fraction can grow by a factor of up to 5 with respect to the corresponding Gaussian model. The increase of the filling factor has a small impact on the reionization optical depth and is of the order of ~ 10 per cent if a scale-dependent non-Gaussianity is assumed. Our predictions for non-Gaussian models are in agreement with the latest *Wilkinson Microwave Anisotropy Probe* results within the error bars, but a higher precision is required to constrain the scale dependence of non-Gaussianity.

Key words: galaxies: evolution – intergalactic medium – cosmology: theory – early Universe.

1 INTRODUCTION

Reionization marks a crucial event in the history of the Universe when the first sources of ultraviolet (UV) radiation ionize the neutral intergalactic medium (IGM) and affect the subsequent formation of the cosmic structures. When reionization ends, the small amount of left neutral hydrogen is responsible for the absorption lines that we observe today in the spectra of far objects. However, the way in which this complex phenomenon occurs is still not well understood, and the most recent observations paint it as a spatially inhomogeneous and not instantaneous process. While the Gunn & Peterson trough of the high-z quasi-stellar object (QSO) spectra suggests a late epoch of reionization at $z \approx 6$ (Becker et al. 2001; Fan et al. 2001; White et al. 2003; Fan et al. 2006), the very recent analysis of the 5-year *Wilkinson Microwave Anisotropy Probe* (*WMAP*) data

on the cosmic microwave background (CMB) polarization shows an IGM optical depth $\tau \sim 0.084$, which is in better agreement with an earlier reionization redshift, $z \sim 10.8$ (Komatsu et al. 2008). On the other hand, a late reionization end at $z \sim 6$ is also probed by the IGM temperature measured at $z < 4$ (Hui & Haiman 2003) and by the lack of evolution in the luminosity function of Lyman-α galaxies between $z = 5.7$ and 6.5 [Malhotra & Rhoads 2004; see, however, Ota et al. (2008) for evidences of a decline at high redshift]. Overall, the present situation regarding reionization at redshift $z \sim 6$ as probed by QSO spectra is still unclear (Becker, Rauch & Sargent 2007).

Many analytic, semi-analytic and numerical models (see e.g. Gnedin 2000; Ciardi, Ferrara & White 2003b; Haiman & Holder 2003; Wyithe & Loeb 2003; Barkana & Loeb 2004; Madau et al. 2004; Choudhury & Ferrara 2007; Iliev et al. 2007; Wyithe & Cen 2007; Ricotti, Gnedin & Shull 2008) have been proposed to describe this poorly understood reionization process. They basically relate the statistical properties and morphology of the ionized regions to the hierarchical growth of the ionizing sources, making more or less

⋆E-mail: daniela.crociani5@unibo.it (DC); lauro.moscardini@unibo.it (LM); viel@oats.inaf.it (MV); sabino.matarrese@pd.infn.it (SM)

detailed assumptions to describe the ionization and recombination processes acting on the IGM. Since the first sources of UV background radiation appear in the first formed dark matter haloes, which correspond to the highest peaks of the primordial density field, the reionization process is expected to strongly depend on the main parameters describing the cosmological model and the power spectrum of primordial density fluctuations. For instance, the possible presence of an evolving component of dark energy can imprint signatures in the resulting morphology of the ionized regions and change the time-scales of the whole process (see e.g. Maio et al. 2006; Crociani et al. 2008). Also, the nature and the statistical distribution of the primordial matter fluctuations can influence the reionization history. Although the standard scenario for the origin of the structures assumes that the primordial perturbations are adiabatic and have a (almost) Gaussian distribution, small deviations from primordial Gaussianity affect the dark halo counts, in the rare-event tail, thus also in the high peaks of the density field which originated collapsed objects at high z.

The aim of this work is to investigate the effects of some level of non-Gaussianity in the primordial density field on the reionization history. We will make use of analytical techniques to describe the processes in action on the IGM. In particular, we will extend previous works in which the considered non-Gaussian models have density fluctuations described by a renormalized χ^2 probability distribution with ν degrees of freedom (Avelino & Liddle 2006) or by a modified Poisson distribution with a given expectation value λ (Chen et al. 2003). Here, we will adopt a more convenient way to introduce primordial non-Gaussianity, which has now become standard in the literature, based on the parameter f_{NL} (see the next section for its definition). In particular, we will assume two different kinds of non-Gaussianity, characterized by a scale-independent and scale-dependent f_{NL} parameter.

The paper is organized as follows. In Section 2, we introduce the main characteristics of the cosmological models with primordial non-Gaussianity considered here. Section 3 reviews the main assumptions of the analytical model adopted to describe the cosmic reionization process. The main results of our analysis are presented and discussed in Section 4. Finally, in Section 5, we draw our conclusions.

2 MODELLING PRIMORDIAL NON-GAUSSIANITY

The main purpose of this work is to study the process of reionization under the assumption that the formation of the first ionizing sources is driven by the spherical collapse of overdense regions in a non-Gaussian primordial density field. The predicted reionization history will be compared to that obtained assuming the 'standard' model, with a Gaussian distribution of primordial perturbations, that will represent our 'reference' case.

All the models considered in this work share the cosmological parameters suggested by the recent analysis of the 5-year *WMAP* data (Komatsu et al. 2008): a Λ cold dark matter (ΛCDM) cosmology where the contributions to the present density parameter from dark matter, cosmological constant and baryons are $\Omega_{m0} = 0.279$, $\Omega_{\Lambda 0} = 0.7214$, $\Omega_{b0} = 0.0461$, respectively; the Hubble constant (in the units of $100 \, \text{km} \, \text{s}^{-1} \, \text{Mpc}^{-1}$) is $h = 0.701$. The normalization of the CDM power spectrum is fixed by assuming $\sigma_8 = 0.817$ and the primordial spectral index is taken to be $n = 0.96$.

We will describe the level of primordial non-Gaussianity using the dimensionless parameter f_{NL} which weighs the quadratic correction to the linear Gaussian term in Bardeen's gauge-invariant potential Φ:

$$\Phi(\boldsymbol{x}) = \Phi_G(\boldsymbol{x}) + f_{NL} * \left[\Phi_G^2(\boldsymbol{x}) - \langle \Phi_G^2(\boldsymbol{x}) \rangle \right], \qquad (1)$$

where $\Phi_G(\boldsymbol{x})$ is a Gaussian random field and $*$ denotes a convolution. On scales smaller than the Hubble radius, Φ is minus the usual Newtonian gravitational potential. With our convention, a positive value for f_{NL} leads to a positive skewness for the distribution of the matter density fluctuations.

As shown by equation (1), in general the non-Gaussian contribution to the gravitational potential Φ can be written as a convolution between a space- and/or shape-dependent $f_{NL}(\boldsymbol{x})$ and the quadratic term $\Phi_G^2(\boldsymbol{x})$. The possible dependences of f_{NL} are often neglected in the literature: this is done mostly for the sake of simplicity, but it can be motivated by the small rms value of Φ. In this case, the bispectrum of the gravitational potential, defined as

$$\langle \Phi(\boldsymbol{k}_1) \Phi(\boldsymbol{k}_2) \Phi(\boldsymbol{k}_3) \rangle = (2\pi)^3 \delta^3(\boldsymbol{k}_1, \boldsymbol{k}_2, \boldsymbol{k}_3) F_s(k_1, k_2, k_3), \qquad (2)$$

δ^3 being Dirac's delta function, assumes a dependence on the wavenumbers called 'local shape', for which the term $F_s(k_1, k_2, k_3)$ can be expressed as

$$F_s(k_1, k_2, k_3) = 2 f_{NL}[P(k_1)P(k_2) + P(k_1)P(k_3) + P(k_2)P(k_3)]. \qquad (3)$$

In the previous equation, $P(k) \equiv \Delta_\Phi k^{-3+(n-1)}$ represents the normalized power spectrum of Φ. Bispectra which can be expressed as in equation (3) are typical for models where the non-Gaussianity is produced outside the horizon or when the inflaton has a varying decay rate. It can be shown that equation (3) assumes the largest values for squeezed configurations, i.e. when one wavenumber is much smaller than the other two.

Alternative models for primordial non-Gaussianity, based on a single field with higher derivative terms, predict a different shape for the bispectrum having the so-called equilateral shape. Its expression can be still obtained using equation (2), but replacing $F_s(k_1, k_2, k_3)$ as follows (Creminelli et al. 2007):

$$F_s(k_1, k_2, k_3) = 6 f_{NL}(k_1, k_2, k_3) \Delta_\Phi^2 \left[- \frac{(k_1 k_2)^{n-1}}{(k_1 k_2)^3} + 2 \, \text{perm} \right.$$

$$- \frac{2(k_1 k_2 k_3)^{2(n-1)/3}}{(k_1 k_2 k_3)^2} + \frac{\left(k_1^{1/3} k_2^{2/3} k_3 \right)^{(n-1)}}{k_1 k_2^2 k_3^3}$$

$$\left. + 5 \, \text{perm} \right], \qquad (4)$$

where we explicitly write the possible scale dependence of f_{NL}. As its name suggests, in this case the maximum amplitude of the bispectrum is where the wavenumbers are all equal. We refer to Lo Verde et al. (2008) for an extended discussion about the role of bispectrum shapes in the parametrization of primordial non-Gaussianity and Bartolo et al. (2004) for a review on the predictions for f_{NL} in different inflationary models.

At present, the strongest constraints on the parameter f_{NL} are based on CMB data. Analysing the 5-year temperature maps obtained by the satellite *WMAP*, Komatsu et al. (2008) derived $-9 < f_{NL} < 111$ when the local shape for the bispectrum is assumed, and $-151 < f_{NL} < 253$ for the equilateral shape. Both limits have been estimated at the 95 per cent confidence level. The fact that the presence of some amount of primordial non-Gaussianity alters the growth of density fluctuations and then the formation and evolution of cosmic structures suggests that the large-scale structure (LSS) of the universe can be an alternative powerful probe for f_{NL}, which has also the important advantage of being based

mostly on three-dimensional data. Many theoretical studies, based both on analytic and on numerical analyses, have investigated the constraining capability of different observables like the abundances of virialized objects like clusters (Messina et al. 1990; Moscardini et al. 1991; Weinberg & Cole 1992; Matarrese, Verde & Jimenez 2000; Verde et al. 2000; Mathis, Diego & Silk 2004; Grossi et al. 2007; Kang, Norberg & Silk 2007; Lo Verde et al. 2008), halo biasing (Dalal et al. 2008; Matarrese & Verde 2008; McDonald 2008), galaxy bispectrum (Sefusatti & Komatsu 2007), density mass field distribution (Grossi et al. 2008) and topology (Matsubara 2003; Hikage et al. 2008), integrated Sachs–Wolfe effect (Afshordi & Tolley 2008; Carbone, Verde & Matarrese 2008), low-density IGM and the Lyman-α flux (Viel et al. 2008), 21 cm fluctuations (Cooray 2005; Pillepich, Porciani & Matarrese 2007) and reionization as discussed in this paper. In general, the application of these theoretical results to real LSS data provided weaker constraints on $f_{\rm NL}$ with respect to the CMB. The only exception is the very recent analysis made by Slosar et al. (2008), who applied the bias formalism to a compendium of large-scale data, including the spectroscopic and photometric luminous red galaxies from the Sloan Digital Sky Survey (SDSS), the SDSS photometric quasars and the cross-correlation between galaxies and dark matter via integrated Sachs–Wolfe effect. Considering the local shape only, they found $-29 < f_{\rm NL} < 70$ (at 95 per cent confidence level). It is important to note that the scales probed by CMB and LSS are generally different and can give complementary information on $f_{\rm NL}$ if the primordial non-Gaussianity is assumed to be scale dependent (see the discussion in Lo Verde et al. 2008).

In this work, we consider non-Gaussian model with bispectrum having both the local and equilateral shapes. We will use values for $f_{\rm NL}$ in the range constrained by the 5-year *WMAP* results (Komatsu et al. 2008), i.e. $-9 < f_{\rm NL} < 111$ and $-151 < f_{\rm NL} < 253$ for local and equilateral shapes, respectively. In the last case, we also allow the non-Gaussianity to vary with the scale, assuming the dependence proposed by Lo Verde et al. (2008), namely

$$f_{\rm NL}(k_1, k_2, k_3) = f_{\rm NL} \left(\frac{k_1 + k_2 + k_3}{k_{\rm CMB}} \right)^{-2\alpha}. \tag{5}$$

The normalization of the previous relation is chosen in order to avoid violating the *WMAP* constraints: for this reason, $f_{\rm NL}$ represents the equilateral parameter measured on the $k_{\rm CMB}$ scale of $0.086\,h\,{\rm Mpc}^{-1}$, roughly corresponding to largest multipole used by Komatsu et al. (2008) to estimate the non-Gaussianity in the *WMAP* data, $\ell = 700$. The slope α is a free parameter assumed to be constant, such that $|\alpha| \ll 1$ between CMB and cluster scales. Following Lo Verde et al. (2008), we consider small negative values for α to enhance the non-Gaussianity on scales smaller than CMB. The resulting behaviour of the $f_{\rm NL}$ parameter is shown in Fig. 1, where we assume $\alpha = 0, -0.1, -0.2$ for the slope of the scale dependence and $f_{\rm NL} = -151$ and 253 as pivoting values at the CMB scale, in agreement with the *WMAP* equilateral constraints. It is evident from the plot that with our assumption for the scale-dependence relation of non-Gaussianity, the absolute value of $f_{\rm NL}$ at the scales relevant for the halo formation, and then for reionization, can be a factor of 2–3 larger than the maximum amount directly derived from the CMB analysis: this can amplify the possible effects of primordial non-Gaussianity. Furthermore, we note that the possible non-Gaussianity probes also are based on observational data coming from different ranges of redshift.

Deviations from Gaussianity influence the evolution of the density fluctuations and affect the distribution of the virialized dark matter haloes at a given cosmological epoch. This reflects on the
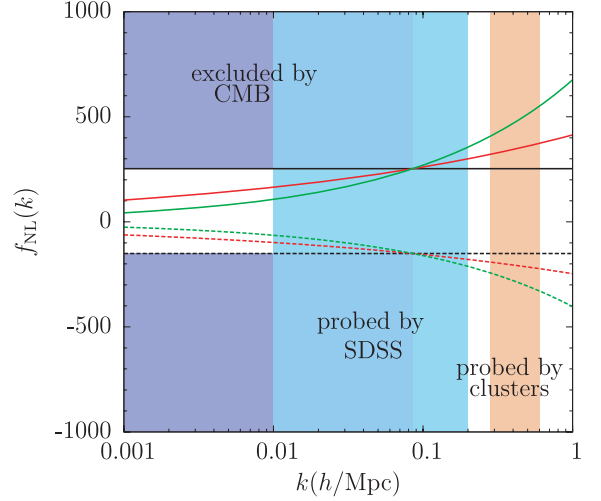

Figure 1. The scale dependence of the non-Gaussianity parameter $f_{\rm NL}$ for the models with equilateral shape considered in this paper. Results for two different choices of the pivoting value, $f_{\rm NL} = -151$ and $f_{\rm NL} = 253$, are shown by dashed and solid curves, respectively. Different values for the slope α have also been used: $\alpha = 0$ (black lines), $\alpha = -0.1$ (red lines) and $\alpha = -0.2$ (green lines). The shaded regions on the right show the scales probed by the SDSS (cyan) and the galaxy clusters (orange), while the blue region refers to the range excluded at 95 per cent confidence level by the CMB data (Komatsu et al. 2008).

mass function: its high-mass tail is enhanced (reduced) in case of positive (negative) values of $f_{\rm NL}$. While in the Gaussian case, the Press & Schechter (1974) (hereafter PS74) approach, together with its modern improvements (Lacey & Cole 1993; Sheth & Tormen 1999; Jenkins et al. 2001; Warren et al. 2006), represents powerful tools to model the evolution of the ionizing sources; for mildly non-Gaussian fields, it is possible to make use of the analytic relation found by Matarrese et al. (2000) extending the PS74 formalism, which has been positively tested against the results of high-resolution N-body simulations by Grossi et al. (2007). If $n_{\rm G}(M, z)$ represents the density of dark matter haloes with mass M at redshift z as obtained assuming Gaussian initial conditions, here modelled assuming the relation found by Sheth & Tormen (1999), the corresponding expression for a non-Gaussian models having the same cosmological parameters can be written as

$$n_{\rm NG}(M, z) = F_{\rm NG}(M, z) n_{\rm G}(M, z), \tag{6}$$

where the correction factor $F_{\rm NG}$ is given by

$$F_{\rm NG}(M, z) \simeq \left| \left[\frac{1}{6} \frac{\delta_{\rm c}^2}{\delta_*} \frac{{\rm d}S_3(M)}{{\rm d}\ln\sigma_{\rm M}} + \frac{\delta_*}{\delta_{\rm c}} \right] \right| \exp\left(\frac{\delta_{\rm c}^3 S_3}{6\sigma_{\rm M}^2} \right). \tag{7}$$

In the previous relation $\delta_* \equiv \delta_{\rm c}\sqrt{1 - S_3(M)\delta_{\rm c}/3}$, $\delta_{\rm c}$ represents the collapse threshold at z, $\sigma_{\rm M}^2$ is the mass variance at $z = 0$ and $S_3(M)$ is the normalized skewness of the primordial density field on mass scale M, namely $S_3(M) = -f_{\rm NL}\mu_3(M)/\sigma_{\rm M}^4$. Then, in order to compute the mass function for non-Gaussian models, it is necessary to evaluate the third-order moment μ_3 that depends on the bispectrum of the gravitational potential $\langle\Phi(\boldsymbol{k}_1)\Phi(\boldsymbol{k}_2)\Phi(\boldsymbol{k}_3)\rangle$:

$$\mu_3(M) = \int \frac{{\rm d}\boldsymbol{k_1}}{(2\pi)^3} \int \frac{{\rm d}\boldsymbol{k_2}}{(2\pi)^3} \int \frac{{\rm d}\boldsymbol{k_3}}{(2\pi)^3}$$
$$\times W(k_1) W(k_2) W(k_3) F(k_1) F(k_2) F(k_3)$$
$$\times \langle\Phi(\boldsymbol{k_1})\Phi(\boldsymbol{k_2})\Phi(\boldsymbol{k_3})\rangle, \tag{8}$$
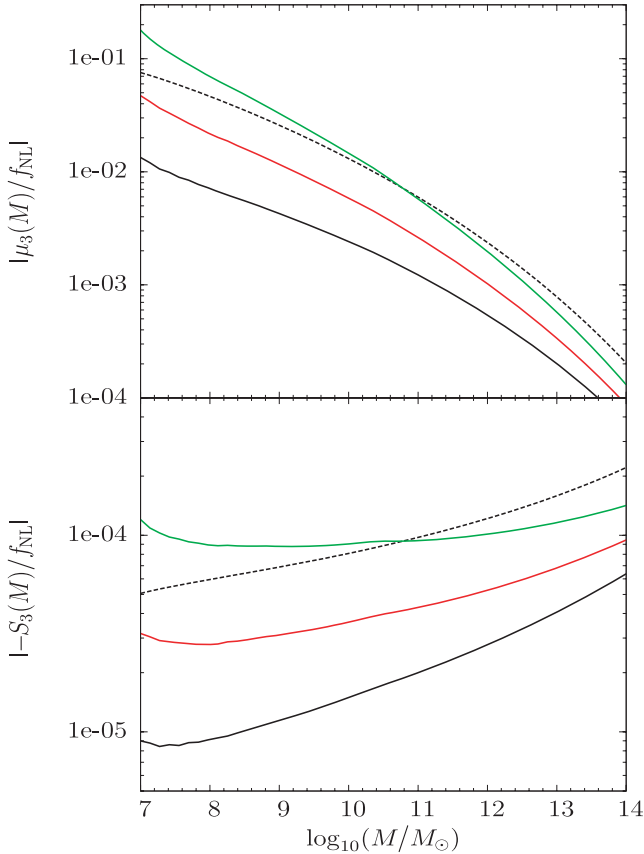
Figure 2. The skewness μ_3 (top panel) and the normalized skewness S_3 (bottom panel) given per unit f_{NL}. The black dashed curve refers to the model with local shape, while the coloured solid curves present the results for the equilateral configuration with $\alpha = 0, -0.1, -0.2$ (black, red and green lines, respectively).

where $W(k)$ is the Fourier transform of a spherical top-hat function on the mass scale M, $F(k) \equiv T(k)g(k)$, being $T(k)$ the CDM transfer function and $g(k) \equiv -2(k/H_0)^2/(3\Omega_{m0})$ is required to go from the gravitational potential to the density via the Poisson equation.

In Fig. 2 we show, as a function of the halo mass, μ_3 and S_3 for models with both local and equilateral shapes. Both skewness parameters are given per unit non-Gaussianity parameter f_{NL}; for the equilateral case, we also consider the possibility of scale dependence for the non-Gaussian term. As already shown by Lo Verde et al. (2008), the two classes of models give quite different predictions for both the amplitude and the mass dependence of the two considered quantities. But this discrepancy decreases as the mass scale increases, since the local and the equilateral cases become more and more similar. The scale dependence of f_{NL} strongly affects the non-Gaussianity contribution for the smaller mass scales and this effect grows when higher negative α parameters are assumed.

Inserting the values for S_3 in equation (7), we can estimate the effects of primordial non-Gaussianity on the dark matter halo distribution at the cosmological epochs relevant for the process of reionization. The results, shown in terms of ratio with respect to the Gaussian predictions, are shown in Fig. 3 for both local and equilateral shapes (upper and lower panels, respectively). Here, we adopt for the f_{NL} parameter at the CMB scale the values corresponding to the 95 per cent confidence level, as derived from the 5-year *WMAP* data: $f_{NL} = -9, 111$ for the local shape and $f_{NL} = -151, 253$ for equilateral one. Since the mass density probability function

is positively skewed in case of positive ($f_{NL} > 0$) non-Gaussian contributions, the probability of overcoming the collapse threshold becomes higher. As a consequence, the formation of high-mass haloes is enhanced and anticipated when $f_{NL} > 0$. Fig. 3 shows that the mass function can be increased by a factor of 10 at $z = 13$ for haloes with mass $M \sim 10^{11}\,M_\odot$ when compared to the standard scenario. We should, however, remark that the high-mass haloes ($M > 10^9\,M_\odot$) at early cosmological epochs are rare events, as shown also by the small number density at $z = 13$ in the reference case, $n(>10^9\,M_\odot) \lesssim 5 \times 10^{-3}\,\mathrm{Mpc}^{-3}$. Then, this effect is expected to have a little impact on the integrated quantities as the total ionized fraction of the IGM optical depth. Unlike the local model, the scale dependence of non-Gaussianity increases the abundance of the low-mass haloes by a factor of ~ 10 at $z = 13$ when compared to the standard case. The opposite applies for $f_{NL} < 0$. As already noted by Matarrese et al. (2000) (see also Verde et al. 2001; Grossi et al. 2007), this effect is more evident at early cosmological epochs, exactly when the process of IGM ionization starts. For this reason, a non-Gaussian distribution of the primordial density field can affect the way in which reionization occurs, leaving its imprints on it, as we will investigate in the next sections.

3 AN ANALYTIC APPROACH TO COSMIC REIONIZATION

In this section, we briefly review the main assumptions underlying the analytic model adopted to describe the process of cosmic reionization. This model is based on the approach proposed by Avelino & Liddle (2006) [see also Haiman & Holder (2003) and Chen et al. (2003) for further details]; our implementation, however, differs in some aspects which will be discussed later.

In this model, the statistical properties of the ionized regions are related to the hierarchical growth of the ionizing sources through simple assumptions on how the galaxies ionize the IGM and on how the IGM recombines. A one-to-one correspondence between the distribution of galaxies and H II regions is established, such that a single galaxy of mass M_{gal} can ionize a region of mass $M_{H\,II} = \zeta M_{gal}$. Here, ζ represents the ionization efficiency of the galaxy, and it is strictly dependent on the nature of the ionizing sources. We will take it as a constant, fixed in such a way that reionization ends at $z = 6.5$.

Since at high redshift the cooling of the gas becomes efficient in haloes having a virial temperature $T \geq 10^4$ K, unlike in Avelino & Liddle (2006), in our analysis we consider only type Ia ($10^4 \leq T \leq 9 \times 10^4$ K) and type Ib ($T > 9 \times 10^4$ K) haloes, neglecting the contribution of the type II sources, which would correspond to haloes with $400 \leq T \leq 10^4$ K. We recall that the distinction between the halo types is related to the way in which they impact the IGM: type Ia sources can grow only in neutral regions, while type Ib haloes can appear also in ionized regions. Consequently, they differently affect the ionization phases of IGM.

The total collapsed fraction $F_{coll}(z)$ at different redshifts can be computed using equation (6):

$$F_{coll}(z) = \frac{1}{\bar{\rho}_0} \int_{M_{min}(z)}^{\infty} \mathrm{d}M\, n_{NG}(M, z)$$
$$= \frac{1}{\bar{\rho}_0} \int_{M_{min}(z)}^{\infty} \mathrm{d}M\, n_G(M, z) F_{NG}(M, z), \qquad (9)$$

where $\bar{\rho}_0$ is the present-day matter density and $M_{min}(z)$ is the minimum mass corresponding to the virial temperature T, which can be computed by inverting the relation proposed by Barkana & Loeb
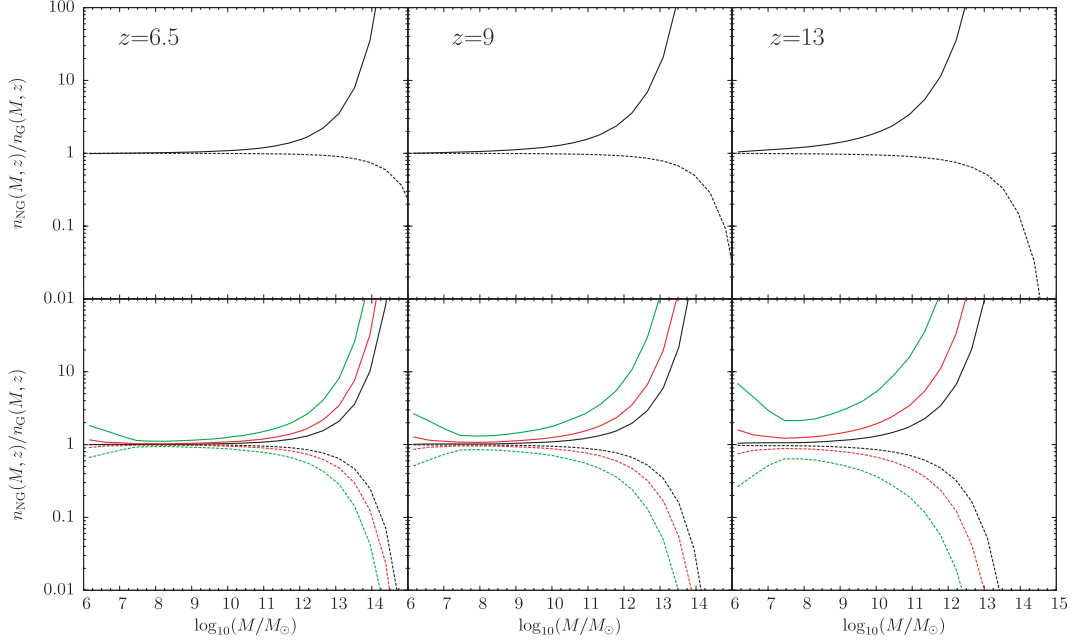
Figure 3. The ratio between the dark matter halo mass functions for non-Gaussian and Gaussian models, computed at $z = 6.5$ (left-hand panels), $z = 9$ (central panels) and $z = 13$ (right-hand panels). Top panels show the results for non-Gaussian models with local shape, where $f_{NL} = -9$ (dashed lines) and $f_{NL} = 111$ (solid lines) are assumed. In the bottom panels, which refer to non-Gaussian models with equilateral shape, dashed and solid lines correspond to $f_{NL} = -151$, 253, respectively; black, red and green lines refer to $\alpha = 0$ (i.e. no scale dependence), $\alpha = -0.1$ and $\alpha = -0.2$, respectively.

(2001), namely

$$T = 1.98 \times 10^4 \left(\frac{1+z}{10} \right) \left(\frac{M}{10^8 \, M_\odot \, h^{-1}} \right)^{2/3} \left(\frac{\Omega_{m0}}{\Omega_m^z} \frac{\Delta_c}{18\pi^2} \right)^{1/3} \text{K}. \tag{10}$$

In the previous equation, Δ_c represents the virial overdensity at redshift z and Ω_m^z is the matter density parameter at redshift z.

Consequently, the collapsed fractions in Ia and Ib haloes are given by

$$F_{coll,Ib}(z) = \frac{1}{\bar{\rho}_0} \int_{M_{min,Ib}(z)}^{\infty} dM \, n_{NG}(M, z),$$

$$F_{coll,Ia}(z) = \frac{1}{\bar{\rho}_0} \int_{M_{min,Ia}(z)}^{\infty} dM \, n_{NG}(M, z) - F_{coll,Ib}(z), \tag{11}$$

where $M_{min,Ib}$ and $M_{min,Ia}$ are the minimum masses for Ib and Ia sources, obtained using equation (10) with $T = 9 \times 10^4$ and 10^4 K, respectively.

The action of the ionizing sources is smoothed down by the recombination of the IGM, here considered as a homogeneous gas. The recombination rate is linearly dependent on the IGM clumping factor $C_{HII} = \langle n_{HII}^2 \rangle / \langle n_{HII} \rangle^2$, for which, following Haiman & Bryan (2006), we assume a redshift evolution modelled as

$$C_{HII}(z) = 1 + 9 \left(\frac{1+z}{7} \right)^{-\beta} \tag{12}$$

being β a free parameter. As shown by Avelino & Liddle (2006), the predicted reionization history of the universe has significant uncertainties introduced by the poor knowledge of the z-dependence of the clumping factor, which cannot be robustly constrained even considering the 3-year *WMAP* results for the reionization optical depth. Since they found good consistency between predicted and observed optical depths irrespective of the amount of primordial non-Gaussianity in the models they consider, we decide to set $\beta = 0$. In this case, the z-dependence of C_{HII} is neglected and

$C_{HII} = 10$. The impact of the assumption of a constant clumping factor will be discussed later.

The probability that a photon emitted at a given cosmological epoch $z_i(t_i)$ is still ionizing at $z < z_i$ can be written as

$$P(t_i, t) = \exp \left(\frac{t_r}{t} - \frac{t_r}{t_i} \right), \tag{13}$$

with $t_r = \alpha_B C_{HII} n_{HI}(t_i) t_i^2$, α_B being the recombination coefficient of H I (=2.6×10^{-13} cm^3 s^{-1} at $T = 10^4$ K) and $n_{HI}(z) = 1.88 \Omega_{b0} h^2 / 0.022 (1 + z)^3$ cm^{-3} the hydrogen density at redshift z. Then, the filling factor $F_{HII}(z)$ at a given cosmological epoch is

$$F_{HII}(z) = \int_{\infty}^{z} dz' \zeta \left\{ \frac{dF_{coll,Ib}}{dz'}(z') + [1 - F_{HII}(z')] \right.$$
$$\left. \times \frac{dF_{coll,Ia}}{dz'}(z') \right\} P(z', z), \tag{14}$$

where the ionizing efficiency is assumed to be the same for the different types of haloes. We note that the different nature of type Ib and Ia sources appears in the right-hand side of equation (14), where the $(1 - F_{HII})$ factor explicitly considers that type Ia haloes form only in neutral regions.

Finally, the H II filling factor allows us to estimate the reionization optical depth as follows:

$$\tau(z) = c\sigma_T \int_t^{t_0} dt' \, n_e(t')$$
$$= 1.08 \, c \, \sigma_T \int_z^0 \frac{dt}{dz'} dz' \left(1 - \frac{3}{4} Y \right) \frac{\rho_b(z')}{m_p} F_{HII}(z'). \tag{15}$$

Here, σ_T represents the cross-section of the Thompson scattering, n_e is the free-electron density, c is the speed of light, Y is the helium mass fraction, $\rho_b(z)$ is the baryon density at redshift z and a factor of 1.08 approximately accounts for the contribution of the He I

reionization, assuming that the H II and He II fractions are equal and neglecting the effects of the He II to He III phase transition.

4 RESULTS AND DISCUSSION

In this section, we present and discuss the main results of the application of the previous model under the assumption that the structure formation history is starting from a primordial non-Gaussian density field. The corresponding predictions will be compared to the reionization scenario obtained for the Gaussian 'reference' case.

First of all, using the minimum collapsed mass at each cosmological epoch as derived from the *M–T* relation proposed by Barkana & Loeb (2001), we can compute the total collapsed fractions for different kinds of sources, following equation (11). The results are presented in Fig. 4, where we show the collapsed fractions of Ia and Ib haloes for the local and the equilateral cases considered here and their redshift evolution compared to the predictions for the Gaussian scenario. We can note that for both the local and the equilateral models, positive values for f_{NL} produce an enhancement of the collapsed fraction at a fixed redshift, given the larger probability for high-mass haloes in the primordial distribution. When scale-dependent non-Gaussianity is considered, this effect becomes
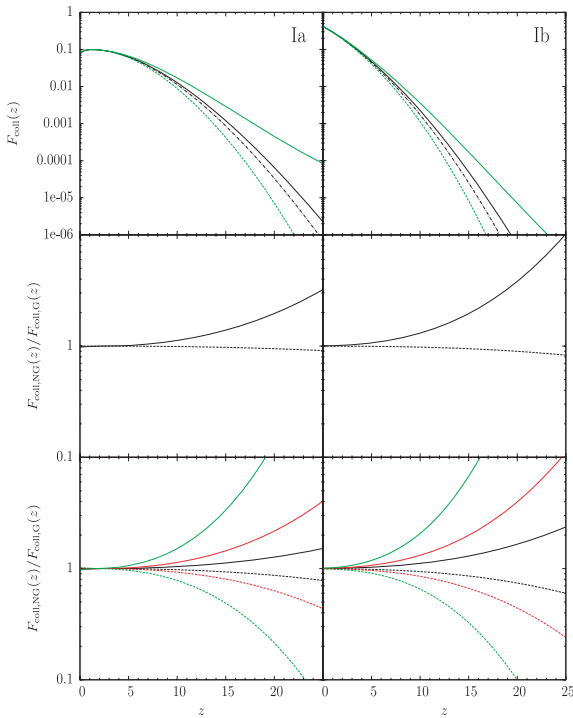

Figure 4. The collapsed fraction of Ia and Ib ionizing sources. The top panels show the resulting F_{coll} for the Gaussian reference case (dot–dashed line) and two extreme non-Gaussian models here considered, which adopt $f_{NL} = 111$ with the local shape (solid line) and $f_{NL} = -151, 253$ with $\alpha = -0.2$ for the equilateral shape (green dotted and solid curves, respectively). The other panels show the ratio between the collapsed fractions of Ia (left-hand panels) and Ib (right-hand panels) ionizing sources for non-Gaussian and Gaussian models as a function of redshift. In the middle panels, the results for non-Gaussian models with local shape are shown where $f_{NL} = -9$ (dashed lines) and $f_{NL} = 111$ (solid lines) are assumed. In the bottom panels, which refer to non-Gaussian models with equilateral shape, dashed and solid lines correspond to $f_{NL} = -151, 253$, respectively; black, red and green lines refer to $\alpha = 0$ (i.e. no scale dependence), $\alpha = -0.1$ and -0.2, respectively.

higher as the power-law parameter α decreases. The opposite trend is observed when negative f_{NL} values are assumed: in this case, we obtain a reduction of the non-Gaussian collapsed fraction due to the smaller probability for high-mass haloes at high z.

The evolution of the collapsed fraction due to non-Gaussianity strongly affects the amount of ionized IGM at different cosmological epochs. As illustrated in Fig. 5, that shows the evolution of the filling factor both for local and for equilateral models, a positive primordial non-Gaussianity produces, if a scale-dependent f_{NL} parameter is assumed, an increase of the ionized IGM density that can become five times higher than that predicted in the Gaussian case. The IGM reionization is slower when negative values are considered, since the smaller collapsed fraction produces a mild evolution of the filling factor, that is smaller compared to the Gaussian case, at every cosmological epoch.

Finally, in Fig. 6 we show the effects of the primordial non-Gaussianity on the reionization optical depth τ assuming both local and equilateral models. As a consequence of the evolution of the ionized fraction, in the initial phases of reionization, the values of τ for the models with positive f_{NL} are higher than those predicted for the Gaussian case. In particular, when a scale-dependent non-Gaussianity is assumed, the change in τ is higher than 10 per cent for $\alpha < -0.2$. In this case, the non-Gaussian optical depth would be $\tau \sim 0.083$ at $z \sim 30$, that is still consistent with the last *WMAP* observations ($\tau = 0.084 \pm 0.016$). Assuming a local shape with largest positive f_{NL} considered here, we find $\tau \sim 0.079$. Note that for the Gaussian model we predict a reionization optical depth at $z = 30 \tau = 0.078$.

We note that our results are in qualitative agreement with the reionization picture resulting from the analysis performed by Chen et al. (2003). However, a direct comparison cannot be done because of the differences in the considered cosmological parameters: in particular, they assume the ones suggested by the first-year *WMAP* analysis, with a significantly higher power spectrum normalization ($\sigma_8 = 0.9$). Furthermore, they parametrize the degree of non-Gaussianity using the expectation value of the considered modified Poisson distribution λ, that is inversely proportional to the f_{NL} parameter used here: $\lambda \propto 1/f_{NL}$. Their results show that a high amount of primordial non-Gaussianity (small λ, i.e. high f_{NL}) produces large deviations with respect to the Gaussian case in the ionized fraction and the IGM optical depth in agreement with our results. We should, however, note that for the Gaussian reference model, the estimate of τ in Chen et al. (2003) differs by 20 per cent with respect to the value we predict using the 5-year *WMAP* cosmology.

The predicted reionization optical depth (at $z = 30$) as a function of the non-Gaussianity parameter f_{NL} is shown in Fig. 7 for the local and equilateral cases. Indeed, the standard deviation on the current estimate of τ from the last *WMAP* results (~ 20 per cent) does not allow us to strictly constrain the scale dependence of non-Gaussianity and, as shown by Liguori & Riotto (2008), should affect the f_{NL} value by a ~ 3 and ~ 5 per cent uncertainty for the local and equilateral shapes, respectively. We estimate that in order to distinguish among different scale dependences, a precision between ~ 1 per cent ($f_{NL} < 0$) and ~ 8 per cent ($f_{NL} > 0$) on the τ measurement is required using CMB-like experiments. In this sense, the smaller standard deviations expected by Planck (~ 6 per cent) (Mukherjee & Liddle 2008) could better probe the reionization optical depth and would possibly constrain the non-Gaussianity parameter with an uncertainty of ~ 1 and ~ 2 per cent in the local and equilaterals models, respectively. We should, however, keep in mind that the current *WMAP* estimate of τ cited in this paper is affected by
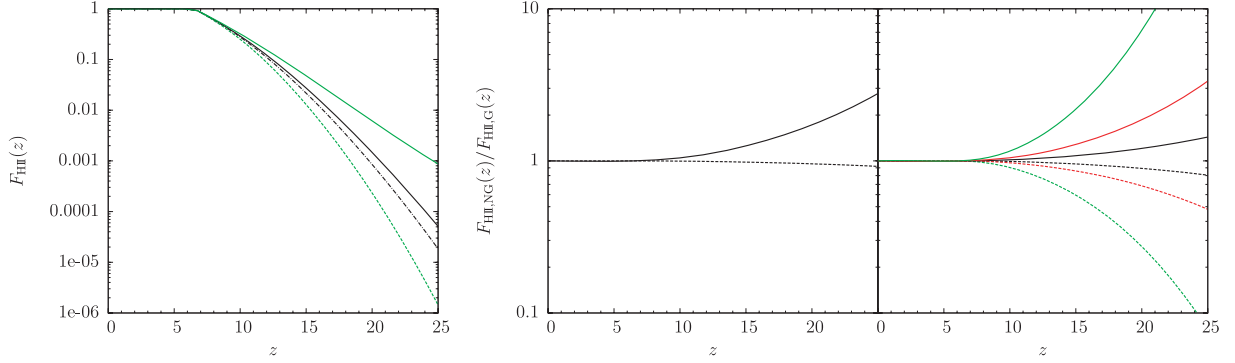
Figure 5. The left-hand panel shows the evolution of the ionized fraction $F_{\mathrm{H\,II}}$ for the Gaussian and two different non-Gaussian models here considered, as in the top panels of Fig. 4. The two panels on the right show the ratio between the ionized fraction $F_{\mathrm{H\,II}}$ for non-Gaussian and Gaussian models as a function of redshift. In the left-hand panel, the results for non-Gaussian models with local shape is shown where $f_{\mathrm{NL}} = -9$ (dashed lines) and $f_{\mathrm{NL}} = 111$ (solid lines) are assumed. In the right-hand panel, which refers to non-Gaussian models with equilateral shape, dashed and solid lines correspond to $f_{\mathrm{NL}} = -151$, 253, respectively; black, red and green lines refer to $\alpha = 0$ (i.e. no scale dependence), $\alpha = -0.1$ and -0.2, respectively.
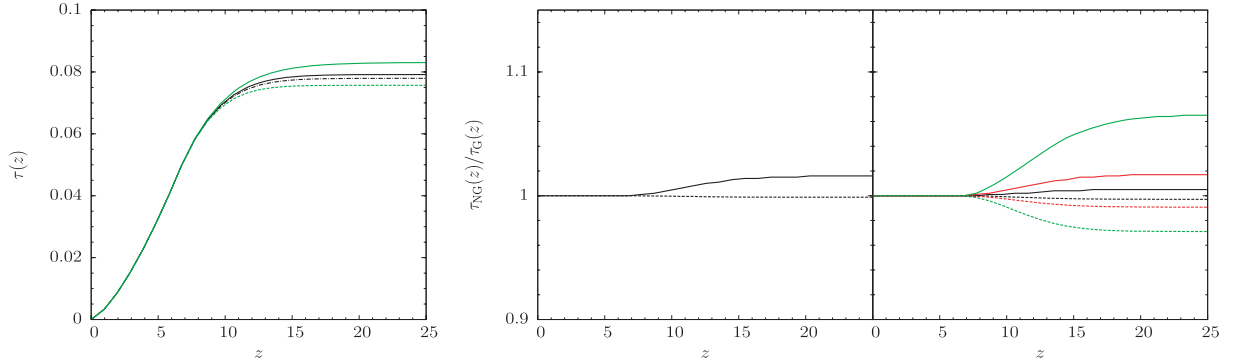

Figure 6. The left-hand panel shows the evolution of the IGM optical depth τ for the Gaussian and two different non-Gaussian models considered here, as in the top panels of Fig. 4. The two panels on the right show the ratio between the reionization optical depth τ for non-Gaussian and Gaussian models as a function of redshift. In the left-hand panel, the results for non-Gaussian models with local shape is shown where $f_{\mathrm{NL}} = -9$ (dashed lines) and $f_{\mathrm{NL}} = 111$ (solid lines) are assumed. In the right-hand panel, which refers to non-Gaussian models with equilateral shape, dashed and solid lines correspond to $f_{\mathrm{NL}} = -151$, 253, respectively; black, red and green lines refer to $\alpha = 0$ (i.e. no scale dependence), $\alpha = -0.1$ and -0.2, respectively.
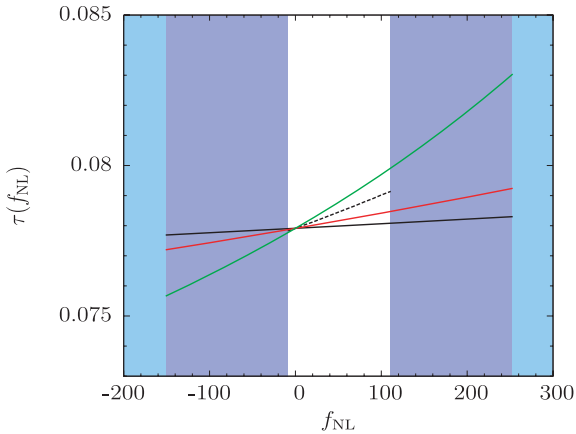

Figure 7. The reionization optical depth τ at redshift $z = 30$ as predicted in different non-Gaussian scenarios is shown as a function of f_{NL}. The dashed black curve refers to the local case, while the solid black, red and green lines correspond to the equilateral case with $\alpha = 0$, -0.1 and -0.2, respectively. The blue and cyan rectangles represent the areas currently excluded by the *WMAP* observations for the local and equilateral cases, respectively.

cosmic variance, since it is based on the bispectrum of the CMB. Recent works investigate alternative methods to avoid this problem (see e.g. Seljak 2008).

As a general warning, we stress that the description of the recombination process in the analytic model adopted here relies on some simplifying assumptions which can affect the way in which reionization occurs. A deeper investigation of the IGM statistical distribution would require the analysis of suitable numerical simulations having non-Gaussian initial conditions. As an example of possible biases introduced by the model uncertainties, in Fig. 8 we show how a time-evolving clumping factor impacts the reionization optical depth. The results have been obtained by setting $\beta = 2$ in equation (12), as suggested by Avelino & Liddle (2006), for which the reionization optical depth is in agreement with the 3-year *WMAP* results for many degrees of non-Gaussianity.

In order to estimate the relative importance of the details of the analytic modelling of the reionization process adopted here, we can compare the IGM optical depths predicted assuming $\beta = 0$ (Fig. 6) and $\beta = 2$ (Fig. 8). As shown by the corresponding left-hand panels, for the Gaussian model the effect on τ due to the change in β and then to the unknown IGM physics is approximately of 10 per cent. Vice versa, considering the non-Gaussian to Gaussian ratios (shown in the right-hand panels of Figs 6 and 8), changing β from 0 to 2
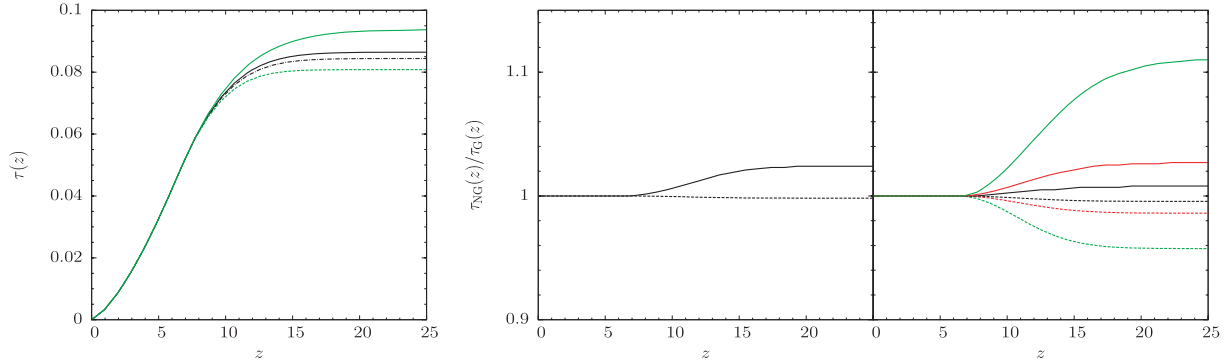
Figure 8. As in Fig. 6, but assuming $\beta = 2$ in the redshift dependence of the clumping factor (see equation 12).

produces negligible effects on the results. In fact, we find that at high z, the ratios obtained with $\beta = 0$ and 2 differ by less than 1 per cent for the mildly non-Gaussian models and by $\sim$4 per cent for the non-Gaussian models with the most extreme scale dependence ($f_{NL} = 253$). By looking at the right-hand panel of Fig. 8, we note that for this last model the effect of introducing a primordial non-Gaussianity can rise up to 10 per cent. This shows that the non-Gaussian to Gaussian ratios are only mildly affected by the choice of the recombination model: this justifies the fact that in this paper we preferred to show most of the results in terms of ratios in spite of absolute values.

Finally, we remark that our approach, which is based on the PS74 formalism and its extensions, cannot fully account for the source clustering that could indeed have relevant effects on the morphology of the H II regions. Since the source distribution depends on the clustering amplitude through the bias parameter, that is different if a primordial non-Gaussianity is considered (see e.g. Carbone et al. 2008; Dalal et al. 2008; Matarrese & Verde 2008), we expect that our results could be affected by this approximation, which can be improved only with suitable numerical simulations.

5 CONCLUSIONS

The aim of this work was to investigate how primordial non-Gaussianity may alter the reionization history when compared to the standard scenario based on Gaussian statistics. We have chosen a simple analytic method to describe the physical processes acting on the IGM to make predictions on the evolution of the ionized fraction and the reionization optical depth. Our work extends previous analyses (Chen et al. 2003; Avelino & Liddle 2006) based on simplified ways to introduce primordial non-Gaussianity, considering models motivated by inflation. In particular, we assume two different hierarchical evolution scenarios for the ionizing sources, characterized by scale-independent and scale-dependent non-Gaussianity. All scenarios considered here are not violating the constraints coming from the recent analysis of the 5-year *WMAP* data.

Our main conclusions can be summarized as follows.

(1) Non-Gaussianity affects the abundance of the dark matter haloes, since the formation of high-mass collapsed objects is enhanced (reduced) when positive (negative) values for the f_{NL} parameter are assumed. This effect is more evident at earlier cosmological epochs, exactly when reionization begins.

(2) As a consequence, for positive primordial non-Gaussianity, the collapsed fraction in type Ia and Ib sources is higher than for

the Gaussian case at the same epoch, and the difference increases with z. The opposite result applies when $f_{NL} < 0$ is assumed.

(3) The IGM filling factor is higher and its evolution is faster than in the Gaussian scenario if a positive f_{NL} is assumed. This effect is enhanced for a scale-dependent non-Gaussianity that can produce a five times higher F_{HII} with respect to the Gaussian case at early cosmological epochs. Vice versa, the filling factor is smaller and has a mild redshift evolution for negative f_{NL}.

(4) Both local and equilateral non-Gaussianity have a small (less than 10 per cent) impact on the reionization optical depth, but the effect is enhanced assuming a scale-dependent f_{NL} parameter.

We finally remark that our predictions of the reionization optical depth in non-Gaussian cosmologies are in agreement with that estimated by 5-yer *WMAP* analysis within 1σ error bars, and a precision higher than that of *WMAP* is required to constrain non-Gaussianity and its scale dependence. Ideally, one would simulate reionization in non-Gaussian cosmological models using hydrodynamical simulations that incorporate all the relevant physical processes in a consistent framework (most importantly radiative transfer effects in the IGM). However, such approach is very time consuming due to the large box size and the high resolution required to simulate large volumes and, at the same time, the physics of the sources of radiation. For this reason, some approximate semi-analytic schemes such as the one presented here are still useful, especially when calibrated on the more robust results of the hydrodynamical runs.

REFERENCES

Afshordi N., Tolley A. J., 2008, Phys. Rev. D, 78, 123507
Avelino P. P., Liddle A. R., 2006, MNRAS, 371, 1755
Barkana R., Loeb A., 2001, Phys. Rep., 349, 125
Barkana R., Loeb A., 2004, ApJ, 609, 474
Bartolo N., Komatsu E., Matarrese S., Riotto A., 2004, Phys. Rep., 402, 103
Becker R. H. et al., 2001, AJ, 122, 2850
Becker G. D., Rauch M., Sargent W. L. W., 2007, ApJ, 662, 72
Carbone C., Verde L., Matarrese S., 2008, ApJ, 684, L1
Chen X., Cooray A., Yoshida N., Sugiyama N., 2003, MNRAS, 346, L31
Choudhury T. R., Ferrara A., 2007, MNRAS, 380, L6

Ciardi B., Ferrara A., White S. D. M., 2003, MNRAS, 344, L7

Cooray A., 2005, MNRAS, 363, 1049

Creminelli P., Senatore L., Zaldarriaga M., Tegmark M., 2007, J. Cosmol. Astropart. Phys., 3, 5

Crociani D., Viel M., Moscardini L., Bartelmann M., Meneghetti M., 2008, MNRAS, 385, 728

Dalal N., Doré O., Huterer D., Shirokov A., 2008, Phys. Rev. D, 77, 123514

Fan X. et al., 2001, AJ, 122, 2833

Fan X. et al., 2006, AJ, 132, 117

Gnedin N. Y., 2000, ApJ, 535, 530

Grossi M., Dolag K., Branchini E., Matarrese S., Moscardini L., 2007, MNRAS, 382, 1261

Grossi M., Branchini E., Dolag K., Matarrese S., Moscardini L., 2008, MNRAS, 390, 438

Haiman Z., Bryan G. L., 2006, ApJ, 650, 7

Haiman Z., Holder G. P., 2003, ApJ, 595, 1

Hikage C., Coles P., Grossi M., Moscardini L., Dolag K., Branchini E., Matarrese S., 2008, MNRAS, 385, 1613

Hui L., Haiman Z., 2003, ApJ, 596, 9

Iliev I. T., Mellema G., Shapiro P. R., Pen U.-L., 2007, MNRAS, 376, 534

Jenkins A., Frenk C. S., White S. D. M., Colberg J. M., Cole S., Evrard A. E., Couchman H. M. P., Yoshida N., 2001, MNRAS, 321, 372

Kang X., Norberg P., Silk J., 2007, MNRAS, 376, 343

Komatsu E. et al., 2008, preprint (astro-ph/0803.0547)

Lacey C., Cole S., 1993, MNRAS, 262, 627

Liguori M., Riotto A., 2008, Phys. Rev. D, 78, 123004

Lo Verde M., Miller A., Shandera S., Verde L., 2008, J. Cosmol. Astropart. Phys., 4, 14

Madau P., Rees M. J., Volonteri M., Haardt F., Oh S. P., 2004, ApJ, 604, 484

Maio U., Dolag K., Meneghetti M., Moscardini L., Yoshida N., Baccigalupi C., Bartelmann M., Perrotta F., 2006, MNRAS, 373, 869

Malhotra S., Rhoads J. E., 2004, ApJ, 617, L5

Matarrese S., Verde L., 2008, ApJ, 677, L77

Matarrese S., Verde L., Jimenez R., 2000, ApJ, 541, 10

Mathis H., Diego J. M., Silk J., 2004, MNRAS, 353, 681

Matsubara T., 2003, ApJ, 584, 1

McDonald P., 2008, Phys. Rev. D, 78, 123519

Messina A., Moscardini L., Lucchin F., Matarrese S., 1990, MNRAS, 245, 244

Moscardini L., Matarrese S., Lucchin F., Messina A., 1991, MNRAS, 248, 424

Mukherjee P., Liddle A. R., 2008, MNRAS, 389, 231

Ota K. et al., 2008, ApJ, 677, 12

Pillepich A., Porciani C., Matarrese S., 2007, ApJ, 662, 1

Press W. H., Schechter P., 1974, ApJ, 187, 425 (PS74)

Ricotti M., Gnedin N. Y., Shull J. M., 2008, ApJ, 685, 21

Sefusatti E., Komatsu E., 2007, Phys. Rev. D, 76, 083004

Seljak U., 2008, preprint (astro-ph/0807.1770)

Sheth R. K., Tormen G., 1999, MNRAS, 308, 119

Slosar A., Hirata C., Seljak U., Ho S., Padmanabhan N., 2008, J. Cosmol. Astropart. Phys., 8, 31

Verde L., Wang L., Heavens A. F., Kamionkowski M., 2000, MNRAS, 313, 141

Verde L., Jimenez R., Kamionkowski M., Matarrese S., 2001, MNRAS, 325, 412

Viel M., Branchini E., Dolag K., Grossi M., Matarrese S., Moscardini L., 2008, MNRAS, in press (arXiv:0811.2223)

Warren M. S., Abazajian K., Holz D. E., Teodoro L., 2006, ApJ, 646, 881

Weinberg D. H., Cole S., 1992, MNRAS, 259, 652

White R. L., Becker R. H., Fan X., Strauss M. A., 2003, AJ, 126, 1

Wyithe J. S. B., Cen R., 2007, ApJ, 659, 890

Wyithe J. S. B., Loeb A., 2003, ApJ, 586, 693

This paper has been typeset from a TEX/LATEX file prepared by the author.